Supplemental Document

Optics EXPRESS

Greatly enhanced photoluminescence of an integrated WSe_2 monolayer by exploiting the pure magnetic resonance and localized strain induced by a hybrid $Si/Si_3N_4/Au$ nanoantenna: supplement

JIANCHENG XU,[1] YUHENG MAO,[1] YESHUN GUO,[1] RUIZHAO YAO,[1] SHULEI LI,[2] HIROSHI SUGIMOTO,[3] MINORU FUJII,[3] FU DENG,[1,4,] GUANGCAN LI,[1] AND SHENG LAN[1,5]

[1] *Guangdong Provincial Key Laboratory of Nanophotonic Functional Materials and Devices, School of Optoelectronic Science and Engineering, South China Normal University, Guangzhou 510006, China*
[2] *School of Optoelectronic Engineering, Guangdong Polytechnic Normal University, Guangzhou 510665, China*
[3] *Department of Electrical and Electronic Engineering, Graduate School of Engineering, Kobe University, Kobe 657-8501, Japan*
[4] *dengfu@m.scnu.edu.cn*
[5] *slan@scnu.edu.cn*

Supplement DOI: https://doi.org/10.6084/m9.figshare.30962246

Parent Article DOI: https://doi.org/10.1364/OE.581332

Greatly enhanced photoluminescence of an integrated WSe_2 monolayer by exploiting the pure magnetic resonance and localized strain induced by a hybrid $Si/Si_3N_4/Au$ nanoantenna

1. Modifications of electromagnetic field distributions in Si NSs

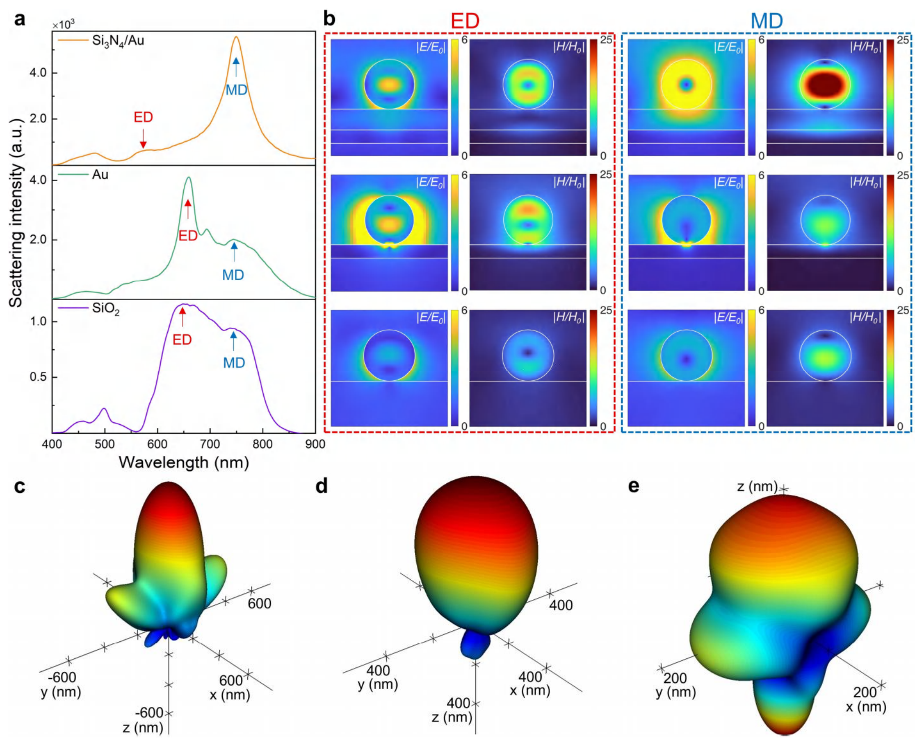

Fig. S1. Modifications of electromagnetic near- and far-field responses of Si NSs on different substrates. (a) Experimental backward scattering spectra of hybrid $Si/Si_3N_4/Au$ nanoantenna with d = 80 nm. For comparison, spectra on the bare Au film and SiO_2 substrate are also shown. Red and blue arrows denote the ED and MD resonances, respectively. (b) Simulated electric- and magnetic-field distributions of Si NSs on Si_3N_4/Au, Au, and SiO_2 substrates at the ED (red box) and MD (blue box) resonances. (c–e) Far-field 3D radiation patterns of Si NSs at the MD resonance on (c) Si_3N_4/Au, (d) Au, and (e) SiO_2 substrates.

2. Scattering characteristics of Si NSs with a radius of 75 nm on Si_3N_4/Au substates

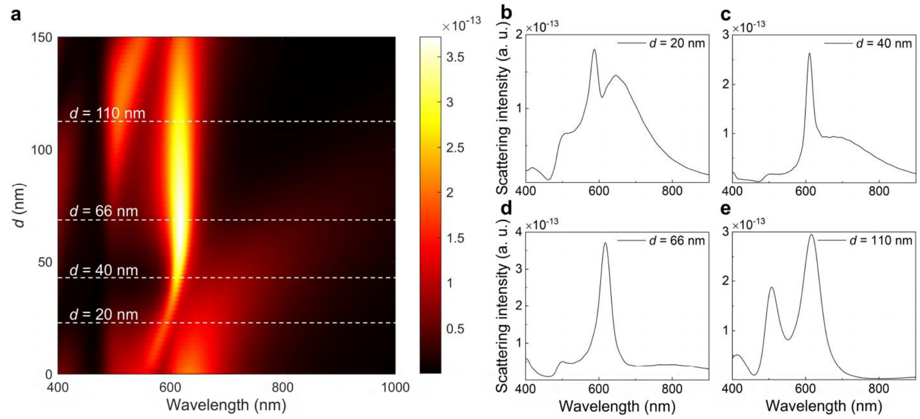

Fig. S2. Scattering characteristics of Si NSs with a radius of 75 nm on Si_3N_4/Au substrates with varying Si_3N_4 thicknesses. (a) Simulated scattering spectra of hybrid Si/Si_3N_4/Au nanoantenna with spacer thicknesses ranging from 0 to 150 nm. The resonant peaks are primarily concentrated within 450–650 nm, demonstrating that tuning the Si_3N_4 thickness enables modulation across the entire visible regime. Four representative thickness values are indicated by white dashed lines. (b–e) Corresponding scattering spectra of Si NSs on Si_3N_4/Au hybrid substrates with spacer thicknesses of (b) 20 nm, (c) 40 nm, (d) 66 nm, and (e) 80 nm.

3. Appearance of hybrid WSe_2/Si/Si_3N_4/Au nanoantennas

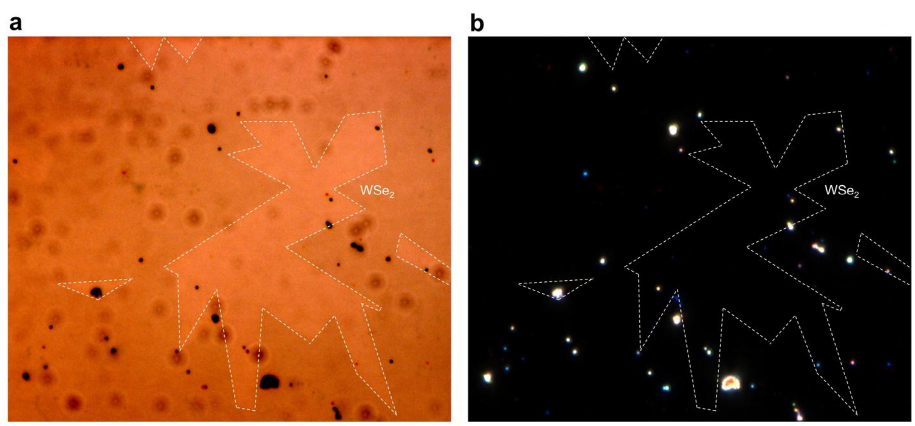

Fig. S3. Bright- and dark-field microscopy of hybrid WSe_2/Si/Si_3N_4/Au nanoantennas. (a) Bright-field image with a Si_3N_4 spacer thickness of 100 nm, showing triangular WSe_2 monolayer flakes and underlying Si NSs. (b) Dark-field image of the same region, where Si NSs with different radii exhibit colorful scattering.

4. Simulation model of the $Si/Si_3N_4/Au$ nanoantenna for Purcell factor enhancement

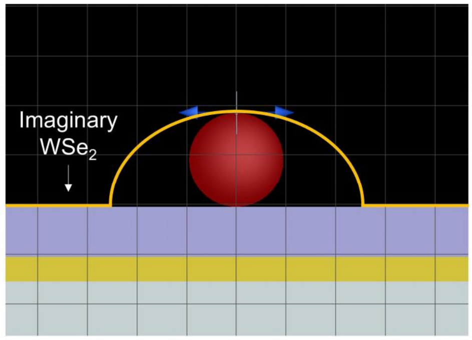

Fig. S4. Simulated Purcell factor of the hybrid $Si/Si_3N_4/Au$ nanoantenna using FDTD. Simulation model of the hybrid nanoantenna with a Si_3N_4 spacer thickness of 100 nm, constructed in FDTD Solutions. An electric dipole was placed above the Si NS to emulate the emission of a WSe_2 monolayer.

5. Lorentz fitting and Voigt fitting of excitons and trions

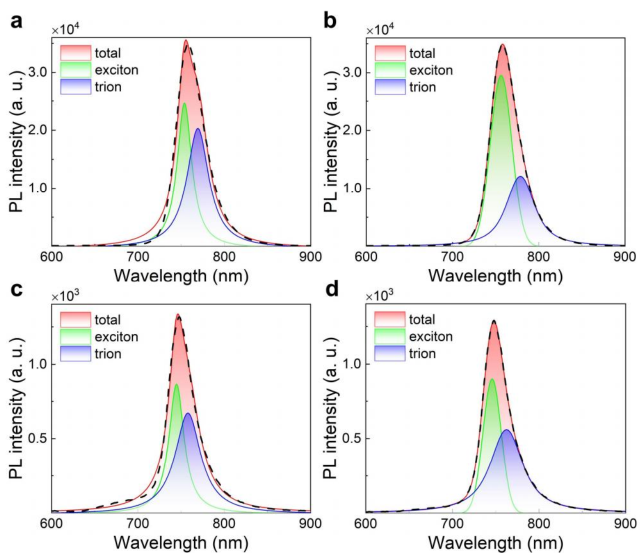

Fig. S5. (a,b) Lorentzian (a) and Voigt (b) fittings of the exciton and trion peaks in the PL spectrum corresponding to Fig. 5a of the main text, measured at an excitation power of 1 mW. (c,d) Lorentzian (c) and Voigt (d) fittings of the exciton and trion peaks in the PL spectrum corresponding to Fig. 5d of the main text, also measured at an excitation power of 1 mW. In all panels, the dashed curves denote the experimentally measured spectra.